JOURNAL OF AIRCRAFT
Vol. 39, No. 6, November–December 2002

Aircraft Small-Disturbance Theory with Longitudinal–Lateral Coupling

W. F. Phillips* and B. W. Santana†
Utah State University, Logan, Utah 84322-4130

The linearized aircraft equations of motion are presented in a form that is more general than the classical uncoupled longitudinal and lateral formulations. The effects of inertial, gyroscopic, and aerodynamic coupling, as well as turning flight, are included. The formulation is presented in both dimensional and nondimensional form. Example results are presented that show that longitudinal–lateral coupling can significantly affect the classical modes of a propeller-driven airplane with high power-to-weight ratio. Predictions from this formulation are consistent with those from the classical formulation, when the coupling terms and bank angle are set to zero. Computation time is not significantly increased over that required for the classical formulation.

Nomenclature

$b_w, \bar{c}_w, S_w$	=	span, mean chord, and planform area of the wing
C_ℓ, C_m, C_n	=	aerodynamic moment coefficients, including thrust (roll, pitch, and yaw components)
C_X, C_Y, C_Z	=	aerodynamic force coefficients, including thrust (x, y, and z components)
$C_{Z,\bar{q}}$	=	example nondimensional aerodynamic derivative, change in C_Z with $\bar{q}$
$C_\theta, S_\theta, T_\theta$	=	shorthand trigonometric notation ($\cos\theta$, $\sin\theta$, and $\tan\theta$)
h_x, h_y, h_y	=	body-fixed angular momentum of spinning rotors (x, y, and z components)
I_{xx}, I_{yy}, I_{zz}	=	body-fixed moment of inertia components
I_{xy}, I_{xz}, I_{yz}	=	body-fixed product of inertia components
l_{ref}	=	congruous aircraft reference length
ℓ, m, n	=	aerodynamic moments, including thrust (roll, pitch, and yaw components)
p, q, r	=	body-fixed angular velocities (roll, pitch, and yaw components)
$\bar{p}, \bar{q}, \bar{r}$	=	traditional nondimensional angular velocities ($pb_w/2V_0$, $q\bar{c}_w/2V_0$, and $rb_w/2V_0$)
$\check{p}, \check{q}, \check{r}$	=	congruous nondimensional angular velocities (pl_{ref}/V_0, ql_{ref}/V_0, and rl_{ref}/V_0)
t	=	time
u, v, w	=	body-fixed translational velocities (x, y, and z components)
V_{wx}, V_{wy}, V_{wz}	=	Earth-fixed wind velocities (x_f, y_f, and z_f components)
V_0	=	equilibrium airspeed
W, g	=	gross aircraft weight and acceleration of gravity
X, Y, Z	=	aerodynamic forces, including thrust (x, y, and z components)
x, y, z	=	body-fixed Cartesian coordinates (forward, right, and downward components)
x_f, y_f, z_f	=	Earth-fixed Cartesian coordinates (north, east, and downward components)
$Z_{,q}$	=	example dimensional aerodynamic derivative, change in Z with q
α, β, μ	=	angle of attack, w/V_0; sideslip angle, v/V_0; and nondimensional forward velocity, u/V_0
$\hat{\alpha}, \hat{\beta}, \hat{\mu}$	=	traditional nondimensional accelerations ($\dot{\alpha}\bar{c}_w/2V_0$, $\dot{\beta}b_w/2V_0$, and $\dot{\mu}\bar{c}_w/2V_0$)
α', β', μ'	=	congruous nondimensional accelerations ($\dot{\alpha}l_{\text{ref}}/V_0$, $\dot{\beta}l_{\text{ref}}/V_0$, and $\dot{\mu}l_{\text{ref}}/V_0$)
Δ	=	deviation from equilibrium
$\delta_a, \delta_e, \delta_r$	=	aileron, elevator, and rudder deflections
ρ, Ω	=	air density and equilibrium turning rate
$\varsigma_x, \varsigma_y, \varsigma_z$	=	nondimensional aircraft position components
ϕ, θ, ψ	=	Euler angles (bank angle, elevation angle, and azimuth angle)

Introduction

FOR aircraft flight mechanics analysis, the six degree-of-freedom (6-DOF) rigid-body equations of motion are commonly linearized using small-disturbance theory.[1–5] In the frequent application of this theory, the lateral equations of motion are uncoupled from the longitudinal equations of motion as a result of imposing the small-disturbance approximation. The actual response of a rigid aircraft to a finite lateral disturbance involves all six DOF. Furthermore, inertial and gyroscopic effects can produce coupling between the lateral and longitudinal equations, even within the framework of small-disturbance theory. What is normally referred to as inertial coupling occurs whenever the aircraft's mass is not completely symmetric about the x–z plane and the so-called gyroscopic coupling occurs as a result of any net angular momentum associated with rotors spinning relative to the body-fixed coordinate system. Aircraft asymmetry can also give rise to aerodynamic coupling because aerodynamic derivatives such as $C_{\ell,\alpha}$, $C_{n,\alpha}$, and $C_{m,\beta}$ can become nonzero. Even in current aircraft, the occurrence of such first-order coupling between the longitudinal and lateral DOF is not unusual. Furthermore, this coupling could prove to be particularly important in the relatively new field of microflight, where the propulsion system rotor mass may be a very significant fraction of the total aircraft mass. However, such coupling is not accounted for in the usual linearized aircraft stability and control analysis.

Uncoupling the longitudinal and lateral equations of motion reduces the eigenproblem associated with linearized 6-DOF aircraft dynamics from one 12×12 system to two 6×6 systems. Decades ago, when the theory of linearized aircraft dynamics was first developed,[6] this represented a significant reduction in computational effort. To reduce computations even further, each of these 6×6 systems was commonly reduced algebraically to a 4×4 system. The eigenvalues obtained from the 4×4 system are identical

Received 29 November 2001; revision received 28 May 2002; accepted for publication 29 June 2002.

*Professor, Mechanical and Aerospace Engineering Department. Member AIAA.
†Adjunct Professor, Mechanical and Aerospace Engineering Department.

to those obtained from the 6×6 system, except that the lower-order system does not yield the trivial rigid-body displacement modes. This represents no loss of information. However, there is a loss of information in the eigenvectors when the 6×6 systems are reduced to 4×4. Two components of each eigenvector are lost. This was a small price to pay for the computational savings that were realized in the early- to mid-20th century.

Today, there are no significant computational savings to be gained by uncoupling the linearized longitudinal and lateral equations of motion. When modern computational facilities are used, the solution of a 12×12 eigenproblem is trivial. Thus, it is quite simple to account for longitudinal–lateral coupling in linearized 6-DOF aircraft dynamics.

Formulation

The traditional Euler angle formulation of the rigid-body 6-DOF equations of motion can easily be modified to account for the effects of longitudinal–lateral coupling.[7,8] Thus, including the effects of gyroscopic and inertial coupling, the 12 first-order differential equations that govern the motion of a rigid aircraft can be written as

$$\frac{W}{g}\begin{Bmatrix}\dot{u}\\ \dot{v}\\ \dot{w}\end{Bmatrix} = \begin{Bmatrix}X\\ Y\\ Z\end{Bmatrix} + W\begin{Bmatrix}-S_\theta\\ S_\phi C_\theta\\ C_\phi C_\theta\end{Bmatrix} + \frac{W}{g}\begin{Bmatrix}rv - qw\\ pw - ru\\ qu - pv\end{Bmatrix} \tag{1}$$

$$\begin{bmatrix} I_{xx} & -I_{xy} & -I_{xz}\\ -I_{xy} & I_{yy} & -I_{yz}\\ -I_{xz} & -I_{yz} & I_{zz}\end{bmatrix}\begin{Bmatrix}\dot{p}\\ \dot{q}\\ \dot{r}\end{Bmatrix} = \begin{Bmatrix}\ell\\ m\\ n\end{Bmatrix} + \begin{bmatrix}0 & -h_z & h_y\\ h_z & 0 & -h_x\\ -h_y & h_x & 0\end{bmatrix}\begin{Bmatrix}p\\ q\\ r\end{Bmatrix} + \begin{Bmatrix}(I_{yy} - I_{zz})qr + I_{yz}(q^2 - r^2) + I_{xz}pq - I_{xy}pr\\ (I_{zz} - I_{xx})pr + I_{xz}(r^2 - p^2) + I_{xy}qr - I_{yz}pq\\ (I_{xx} - I_{yy})pq + I_{xy}(p^2 - q^2) + I_{yz}pr - I_{xz}qr\end{Bmatrix} \tag{2}$$

$$\begin{Bmatrix}\dot{x}_f\\ \dot{y}_f\\ \dot{z}_f\end{Bmatrix} = \begin{bmatrix}C_\theta C_\psi & S_\phi S_\theta C_\psi - C_\phi S_\psi & C_\phi S_\theta C_\psi + S_\phi S_\psi\\ C_\theta S_\psi & S_\phi S_\theta S_\psi + C_\phi C_\psi & C_\phi S_\theta S_\psi - S_\phi C_\psi\\ -S_\theta & S_\phi C_\theta & C_\phi C_\theta\end{bmatrix}\begin{Bmatrix}u\\ v\\ w\end{Bmatrix} + \begin{Bmatrix}V_{wx}\\ V_{wy}\\ V_{wz}\end{Bmatrix} \tag{3}$$

$$\begin{Bmatrix}\dot{\phi}\\ \dot{\theta}\\ \dot{\psi}\end{Bmatrix} = \begin{bmatrix}1 & S_\phi S_\theta / C_\theta & C_\phi S_\theta / C_\theta\\ 0 & C_\phi & -S_\phi\\ 0 & S_\phi / C_\theta & C_\phi / C_\theta\end{bmatrix}\begin{Bmatrix}p\\ q\\ r\end{Bmatrix} \tag{4}$$

where the dot indicates a time derivative.

To obtain the classical dynamic modes from these 12 equations, the system must be linearized relative to some equilibrium flight condition. The equilibrium flight condition commonly chosen for this purpose is steady climbing flight.[1–5] This condition is chosen specifically to eliminate the coupling between the longitudinal and lateral modes. However, this is not the most general equilibrium flight condition that can be used to linearize the equations of motion, if we are willing to accept longitudinal–lateral coupling in the final result.

Perhaps the most common cause of longitudinal–lateral coupling is simple turning flight. The equations of motion are usually linearized relative to a flight path having both the equilibrium bank angle and azimuth angle set to zero. Because there is no force in body-fixed coordinates that depends on azimuth angle, the choice of equilibrium azimuth angle is arbitrary and has no effect on the disturbance equations. On the other hand, allowing for a nonzero equilibrium bank angle will significantly affect the disturbance equations, introducing longitudinal–lateral coupling.

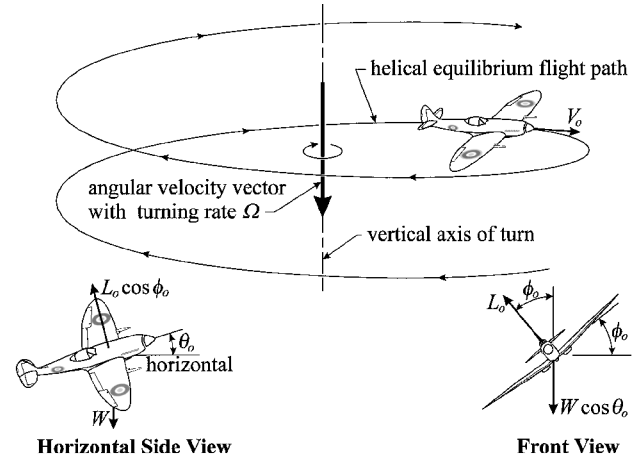

Fig. 1 Equilibrium flight conditions for a steady coordinated turn.

For example, consider the steady coordinated turn shown in Fig. 1. In a steady coordinated turn, the ailerons, elevator, and rudder are coordinated to maintain constant airspeed and angular acceleration while eliminating the side force. The equilibrium angular velocity vector is aligned with the Earth-fixed z_f-axis and, by our choice of the body-fixed coordinate system, the equilibrium translational velocity vector is aligned with the body-fixed x-axis. The equilibrium angular velocity vector in body-fixed coordinates can be determined by applying the usual Earth-fixed to body-fixed transformation matrix[9] to the angular velocity vector in Earth-fixed coordinates,

$$\begin{Bmatrix}p\\ q\\ r\end{Bmatrix}_0 = \begin{bmatrix}C_\theta C_\psi & C_\theta S_\psi & -S_\theta\\ S_\phi S_\theta C_\psi - C_\phi S_\psi & S_\phi S_\theta S_\psi + C_\phi C_\psi & S_\phi C_\theta\\ C_\phi S_\theta C_\psi + S_\phi S_\psi & C_\phi S_\theta S_\psi - S_\phi C_\psi & C_\phi C_\theta\end{bmatrix}\begin{Bmatrix}0\\ 0\\ \Omega\end{Bmatrix}$$

$$= \Omega\begin{Bmatrix}-S_{\theta_0}\\ S_{\phi_0} C_{\theta_0}\\ C_{\phi_0} C_{\theta_0}\end{Bmatrix} \tag{5}$$

where the subscript 0 shall always indicate evaluation at the equilibrium reference state. The translational velocity vector, in body-fixed coordinates, for this equilibrium flight condition and our choice for the body-fixed coordinate system is

$$\begin{Bmatrix}u\\ v\\ w\end{Bmatrix}_0 = \begin{Bmatrix}V_0\\ 0\\ 0\end{Bmatrix} \tag{6}$$

From Eq. (1), constant airspeed and zero side force requires

$$\begin{Bmatrix}0\\ 0\\ 0\end{Bmatrix} = \begin{Bmatrix}X\\ 0\\ Z\end{Bmatrix} + W\begin{Bmatrix}-S_\theta\\ S_\phi C_\theta\\ C_\phi C_\theta\end{Bmatrix} + \frac{W}{g}\begin{Bmatrix}rv - qw\\ pw - ru\\ qu - pv\end{Bmatrix} \tag{7}$$

When Eqs. (5) and (6) are applied to Eq. (7), this equilibrium flight condition gives

$$\begin{Bmatrix}0\\ 0\\ 0\end{Bmatrix} = \begin{Bmatrix}X_0\\ 0\\ Z_0\end{Bmatrix} + W\begin{Bmatrix}-S_{\theta_0}\\ S_{\phi_0} C_{\theta_0}\\ C_{\phi_0} C_{\theta_0}\end{Bmatrix} + \frac{W\Omega V_0}{g}\begin{Bmatrix}0\\ -C_{\phi_0} C_{\theta_0}\\ S_{\phi_0} C_{\theta_0}\end{Bmatrix} \tag{8}$$

From row 2 of Eq. (8), we can determine the equilibrium turning rate as a function of airspeed and bank angle,

$$\Omega = g \tan\phi_0 / V_0 \tag{9}$$

From Eqs. (8) and (9), the net equilibrium aerodynamic force required to maintain a steady coordinated turn is

$$\begin{Bmatrix}X\\ Y\\ Z\end{Bmatrix}_0 = W\begin{Bmatrix}S_{\theta_0}\\ 0\\ -C_{\theta_0}/C_{\phi_0}\end{Bmatrix} \tag{10}$$

From Eqs. (4) and (5), the equilibrium Euler angle rates are readily found to be

$$\begin{Bmatrix} \dot{\phi} \\ \dot{\theta} \\ \dot{\psi} \end{Bmatrix}_0 = \begin{Bmatrix} 0 \\ 0 \\ \Omega \end{Bmatrix} \tag{11}$$

Integrating Eq. (11) subject to the initial condition of zero azimuth angle at time $t = 0$, we find that the equilibrium Euler angles for a steady coordinated turn are

$$\begin{Bmatrix} \phi \\ \theta \\ \psi \end{Bmatrix}_0 = \begin{Bmatrix} \phi_0 \\ \theta_0 \\ \Omega t \end{Bmatrix} \tag{12}$$

Similarly, using this result in Eq. (3) and integrating, the equilibrium position for the steady coordinated turn is

$$\begin{Bmatrix} x_f \\ y_f \\ z_f \end{Bmatrix}_0 = \begin{Bmatrix} V_{wx}t + V_0 C_{\theta_0} S_{\Omega t} / \Omega \\ V_{wy}t - V_0 C_{\theta_0} C_{\Omega t} / \Omega \\ \left(V_{wz} - V_0 S_{\theta_0}\right)t \end{Bmatrix} \tag{13}$$

Expanding the aircraft flight variables relative to this equilibrium state, we have

$$u = V_0 + \Delta u, \qquad v = \Delta v, \qquad w = \Delta w$$

$$p = -g T_{\phi_0} S_{\theta_0} / V_0 + \Delta p, \qquad q = g T_{\phi_0} S_{\phi_0} C_{\theta_0} / V_0 + \Delta q$$

$$r = g S_{\phi_0} C_{\theta_0} / V_0 + \Delta r, \qquad X = W S_{\theta_0} + \Delta X, \qquad Y = \Delta Y$$

$$Z = -W C_{\theta_0} / C_{\phi_0} + \Delta Z, \qquad \ell = \ell_0 + \Delta \ell, \qquad m = m_0 + \Delta m$$

$$n = n_0 + \Delta n, \qquad x_f = V_{wx}t + V_0 C_{\theta_0} S_{\Omega t} / \Omega + \Delta x_f$$

$$y_f = V_{wy}t - V_0 C_{\theta_0} C_{\Omega t} / \Omega + \Delta y_f$$

$$z_f = \left(V_{wz} - V_0 S_{\theta_0}\right)t + \Delta z_f$$

$$\phi = \phi_0 + \Delta\phi, \qquad \theta = \theta_0 + \Delta\theta, \qquad \psi = \Omega t + \Delta\psi$$

where the equilibrium moments are obtained by using these values in Eq. (2) with all disturbances set to zero.

Equations (1–4) can now be linearized, using the steady coordinated turn as an equilibrium reference state. With one exception, the linearization process is straightforward, and most of the details will not be presented here. The useful linearization of Eq. (3) requires a change of variables that has not been commonly used. Thus, some of the details associated with linearizing the kinematic equations for position will be presented.

When the preceding disturbance expansions are used relative to the steady coordinated turn, Eq. (3) can be written as

$$\begin{Bmatrix} V_{wx} + V_0 C_{\theta_0} C_{\Omega t} + \Delta\dot{x}_f \\ V_{wy} + V_0 C_{\theta_0} S_{\Omega t} + \Delta\dot{y}_f \\ V_{wz} - V_0 S_{\theta_0} + \Delta\dot{z}_f \end{Bmatrix} = [[\boldsymbol{T}]_0 + \Delta[\boldsymbol{T}]] \begin{Bmatrix} V_0 + \Delta u \\ \Delta v \\ \Delta w \end{Bmatrix} + \begin{Bmatrix} V_{wx} \\ V_{wy} \\ V_{wz} \end{Bmatrix} \tag{14}$$

where $[\boldsymbol{T}]$ is the transformation matrix,

$$[\boldsymbol{T}] \equiv \begin{bmatrix} C_\theta C_\psi & S_\phi S_\theta C_\psi - C_\phi S_\psi & C_\phi S_\theta C_\psi + S_\phi S_\psi \\ C_\theta S_\psi & S_\phi S_\theta S_\psi + C_\phi C_\psi & C_\phi S_\theta S_\psi - S_\phi C_\psi \\ -S_\theta & S_\phi C_\theta & C_\phi C_\theta \end{bmatrix}$$

$[\boldsymbol{T}]_0$ is its equilibrium value, and $\Delta[\boldsymbol{T}]$ is the change in the transformation matrix that results from the disturbances $\Delta\phi$, $\Delta\theta$, and $\Delta\psi$. When the wind components that appear on both sides of Eq. (14) are eliminated and only first-order terms are retained, Eq. (14) can be written as

$$\begin{Bmatrix} V_0 C_{\theta_0} C_{\Omega t} + \Delta\dot{x}_f \\ V_0 C_{\theta_0} S_{\Omega t} + \Delta\dot{y}_f \\ -V_0 S_{\theta_0} + \Delta\dot{z}_f \end{Bmatrix} = \begin{bmatrix} C_{\theta_0} C_{\Omega t} & S_{\phi_0} S_{\theta_0} C_{\Omega t} - C_{\phi_0} S_{\Omega t} & C_{\phi_0} S_{\theta_0} C_{\Omega t} + S_{\phi_0} S_{\Omega t} \\ C_{\theta_0} S_{\Omega t} & S_{\phi_0} S_{\theta_0} S_{\Omega t} + C_{\phi_0} C_{\Omega t} & C_{\phi_0} S_{\theta_0} S_{\Omega t} - S_{\phi_0} C_{\Omega t} \\ -S_{\theta_0} & S_{\phi_0} C_{\theta_0} & C_{\phi_0} C_{\theta_0} \end{bmatrix} \times \begin{Bmatrix} V_0 + \Delta u \\ \Delta v \\ \Delta w \end{Bmatrix} + \Delta[\boldsymbol{T}] \begin{Bmatrix} V_0 \\ 0 \\ 0 \end{Bmatrix}$$

or

$$\begin{Bmatrix} \Delta\dot{x}_f \\ \Delta\dot{y}_f \\ \Delta\dot{z}_f \end{Bmatrix} = \begin{bmatrix} C_{\theta_0} C_{\Omega t} & S_{\phi_0} S_{\theta_0} C_{\Omega t} - C_{\phi_0} S_{\Omega t} & C_{\phi_0} S_{\theta_0} C_{\Omega t} + S_{\phi_0} S_{\Omega t} \\ C_{\theta_0} S_{\Omega t} & S_{\phi_0} S_{\theta_0} S_{\Omega t} + C_{\phi_0} C_{\Omega t} & C_{\phi_0} S_{\theta_0} S_{\Omega t} - S_{\phi_0} C_{\Omega t} \\ -S_{\theta_0} & S_{\phi_0} C_{\theta_0} & C_{\phi_0} C_{\theta_0} \end{bmatrix} \times \begin{Bmatrix} \Delta u \\ \Delta v \\ \Delta w \end{Bmatrix} + \begin{Bmatrix} -S_{\theta_0} C_{\Omega t} \Delta\theta - C_{\theta_0} S_{\Omega t} \Delta\psi \\ -S_{\theta_0} S_{\Omega t} \Delta\theta + C_{\theta_0} C_{\Omega t} \Delta\psi \\ -C_{\theta_0} \Delta\theta \end{Bmatrix} V_0 \tag{15}$$

Although Eq. (15) may at first appear linear, it is not. All five of the terms on the right-hand side of the first and second rows are sinusoidal functions of time. This 3×3 system can be rearranged to give a linear system by using a change of variables. This requires some algebraic manipulation. The first row in Eq. (15) is replaced with the sum $(C_{\Omega t} \times \text{row}_1 + S_{\Omega t} \times \text{row}_2)$ and the second row is replaced with $(C_{\Omega t} \times \text{row}_2 - S_{\Omega t} \times \text{row}_1)$. When the trigonometric identity $S^2_{\Omega t} + C^2_{\Omega t} = 1$ is applied, this gives

$$\begin{Bmatrix} C_{\Omega t}\Delta\dot{x}_f + S_{\Omega t}\Delta\dot{y}_f \\ C_{\Omega t}\Delta\dot{y}_f - S_{\Omega t}\Delta\dot{x}_f \\ \Delta\dot{z}_f \end{Bmatrix} = \begin{bmatrix} C_{\theta_0} & S_{\phi_0} S_{\theta_0} & C_{\phi_0} S_{\theta_0} \\ 0 & C_{\phi_0} & -S_{\phi_0} \\ -S_{\theta_0} & S_{\phi_0} C_{\theta_0} & C_{\phi_0} C_{\theta_0} \end{bmatrix} \times \begin{Bmatrix} \Delta u \\ \Delta v \\ \Delta w \end{Bmatrix} + \begin{bmatrix} 0 & -V_0 S_{\theta_0} & 0 \\ 0 & 0 & V_0 C_{\theta_0} \\ 0 & -V_0 C_{\theta_0} & 0 \end{bmatrix} \begin{Bmatrix} \Delta\phi \\ \Delta\theta \\ \Delta\psi \end{Bmatrix} \tag{16}$$

The right-hand side of Eq. (16) is now linear in the disturbance variables. Thus, the left-hand side of Eq. (16) suggests using the change of variables

$$\begin{Bmatrix} \Delta\dot{x}_c \\ \Delta\dot{y}_c \\ \Delta\dot{z}_c \end{Bmatrix} \equiv \begin{bmatrix} C_{\Omega t} & S_{\Omega t} & 0 \\ -S_{\Omega t} & C_{\Omega t} & 0 \\ 0 & 0 & 1 \end{bmatrix} \begin{Bmatrix} \Delta\dot{x}_f \\ \Delta\dot{y}_f \\ \Delta\dot{z}_f \end{Bmatrix} \tag{17}$$

These new disturbance variables can be interpreted as the circumferential, radial, and vertical disturbances from the equilibrium coordinated turn. For the special case when the bank angle is zero, these new disturbance variables reduce to the original positional disturbances in Earth-fixed coordinates.

In a similar manner, Eqs. (1), (2), and (4) can be linearized. This gives the general linearized 6-DOF equations of motion for aircraft dynamics,

$$\begin{bmatrix} [\boldsymbol{B}]_m & [\boldsymbol{n}] & [\boldsymbol{n}] & [\boldsymbol{n}] \\ [\boldsymbol{B}]_{iv} & [\boldsymbol{I}] & [\boldsymbol{n}] & [\boldsymbol{n}] \\ [\boldsymbol{n}] & [\boldsymbol{n}] & [\boldsymbol{i}] & [\boldsymbol{n}] \\ [\boldsymbol{n}] & [\boldsymbol{n}] & [\boldsymbol{n}] & [\boldsymbol{i}] \end{bmatrix} \begin{Bmatrix} \Delta\dot{u} \\ \Delta\dot{v} \\ \Delta\dot{w} \\ \Delta\dot{p} \\ \Delta\dot{q} \\ \Delta\dot{r} \\ \Delta\dot{x}_c \\ \Delta\dot{y}_c \\ \Delta\dot{z}_c \\ \Delta\dot{\phi} \\ \Delta\dot{\theta} \\ \Delta\dot{\psi} \end{Bmatrix}$$

$$- \begin{bmatrix} [\boldsymbol{A}]_{fv} & [\boldsymbol{A}]_{f\omega} & [\boldsymbol{n}] & [\boldsymbol{A}]_w \\ [\boldsymbol{A}]_{mv} & [\boldsymbol{A}]_{m\omega} & [\boldsymbol{n}] & [\boldsymbol{n}] \\ [\boldsymbol{A}]_{pv} & [\boldsymbol{n}] & [\boldsymbol{n}] & [\boldsymbol{A}]_{pe} \\ [\boldsymbol{n}] & [\boldsymbol{A}]_{e\omega} & [\boldsymbol{n}] & [\boldsymbol{A}]_{ee} \end{bmatrix} \begin{Bmatrix} \Delta u \\ \Delta v \\ \Delta w \\ \Delta p \\ \Delta q \\ \Delta r \\ \Delta x_c \\ \Delta y_c \\ \Delta z_c \\ \Delta\phi \\ \Delta\theta \\ \Delta\psi \end{Bmatrix}$$

$$= \begin{bmatrix} [\boldsymbol{C}]_f \\ [\boldsymbol{C}]_m \\ [\boldsymbol{n}] \\ [\boldsymbol{n}] \end{bmatrix} \begin{Bmatrix} \Delta\delta_a \\ \Delta\delta_e \\ \Delta\delta_r \end{Bmatrix} \tag{18}$$

where

$$[\boldsymbol{B}]_m = \begin{bmatrix} \frac{W}{g} - X_{,\dot{u}} & 0 & -X_{,\dot{w}} \\ 0 & \frac{W}{g} & 0 \\ -Z_{,\dot{u}} & 0 & \frac{W}{g} - Z_{,\dot{w}} \end{bmatrix}$$

$$[\boldsymbol{B}]_{iv} = \begin{bmatrix} 0 & 0 & 0 \\ -m_{,\dot{u}} & 0 & -m_{,\dot{w}} \\ 0 & 0 & 0 \end{bmatrix}, \qquad [\boldsymbol{I}] = \begin{bmatrix} I_{xx} & -I_{xy} & -I_{xz} \\ -I_{xy} & I_{yy} & -I_{yz} \\ -I_{xz} & -I_{yz} & I_{zz} \end{bmatrix}$$

$$[\boldsymbol{A}]_{fv} = \begin{bmatrix} X_{,u} & \frac{WS_{\phi_0}C_{\theta_0}}{V_0} & X_{,w} - \frac{WT_{\phi_0}S_{\phi_0}C_{\theta_0}}{V_0} \\ -\frac{WS_{\phi_0}C_{\theta_0}}{V_0} & Y_{,v} & -\frac{WT_{\phi_0}S_{\theta_0}}{V_0} \\ Z_{,u} + \frac{WT_{\phi_0}S_{\phi_0}C_{\theta_0}}{V_0} & \frac{WT_{\phi_0}S_{\theta_0}}{V_0} & Z_{,w} \end{bmatrix}$$

$$[\boldsymbol{A}]_{f\omega} = \begin{bmatrix} 0 & X_{,q} & 0 \\ Y_{,p} & 0 & Y_{,r} - \frac{V_0 W}{g} \\ 0 & Z_{,q} + \frac{V_0 W}{g} & 0 \end{bmatrix}$$

$$[\boldsymbol{A}]_w = W \begin{bmatrix} 0 & -C_{\theta_0} & 0 \\ C_{\phi_0}C_{\theta_0} & -S_{\phi_0}S_{\theta_0} & 0 \\ -S_{\phi_0}C_{\theta_0} & -C_{\phi_0}S_{\theta_0} & 0 \end{bmatrix}$$

$$[\boldsymbol{A}]_{mv} = \begin{bmatrix} 0 & \ell_{,v} & \ell_{,w} \\ m_{,u} & m_{,v} & m_{,w} \\ 0 & n_{,v} & n_{,w} \end{bmatrix}, \qquad [\boldsymbol{A}]_{m\omega} = \begin{bmatrix} A_{\ell p} & A_{\ell q} & A_{\ell r} \\ A_{mp} & A_{mq} & A_{mr} \\ A_{np} & A_{nq} & A_{nr} \end{bmatrix}$$

$$A_{\ell p} = \ell_{,p} + \frac{g\left(I_{xz}T_{\phi_0}S_{\phi_0}C_{\theta_0} - I_{xy}S_{\phi_0}C_{\theta_0}\right)}{V_0}$$

$$A_{\ell q} = -h_z + \frac{g\left[(I_{yy} - I_{zz})S_{\phi_0}C_{\theta_0} + 2I_{yz}T_{\phi_0}S_{\phi_0}C_{\theta_0} - I_{xz}T_{\phi_0}S_{\theta_0}\right]}{V_0}$$

$$A_{\ell r} = \ell_{,r} + h_y + \frac{g\left[(I_{yy} - I_{zz})T_{\phi_0}S_{\phi_0}C_{\theta_0} - 2I_{yz}S_{\phi_0}C_{\theta_0} + I_{xy}T_{\phi_0}S_{\theta_0}\right]}{V_0}$$

$$A_{mp} = h_z + \frac{g\left[(I_{zz} - I_{xx})S_{\phi_0}C_{\theta_0} + 2I_{xz}T_{\phi_0}S_{\theta_0} - I_{yz}T_{\phi_0}S_{\phi_0}C_{\theta_0}\right]}{V_0}$$

$$A_{mq} = m_{,q} + \frac{g\left(I_{xy}S_{\phi_0}C_{\theta_0} + I_{yz}T_{\phi_0}S_{\theta_0}\right)}{V_0}$$

$$A_{mr} = -h_x + \frac{g\left[(I_{xx} - I_{zz})T_{\phi_0}S_{\theta_0} + 2I_{xz}S_{\phi_0}C_{\theta_0} + I_{xy}T_{\phi_0}S_{\phi_0}C_{\theta_0}\right]}{V_0}$$

$$A_{np} = n_{,p} - h_y + \frac{g\left[(I_{xx} - I_{yy})T_{\phi_0}S_{\phi_0}C_{\theta_0} - 2I_{xy}T_{\phi_0}S_{\theta_0} + I_{yz}S_{\phi_0}C_{\theta_0}\right]}{V_0}$$

$$A_{nq} = h_x + \frac{g\left[(I_{yy} - I_{xx})T_{\phi_0}S_{\theta_0} - 2I_{xy}T_{\phi_0}S_{\phi_0}C_{\theta_0} - I_{xz}S_{\phi_0}C_{\theta_0}\right]}{V_0}$$

$$A_{nr} = n_{,r} + \frac{g\left(-I_{yz}T_{\phi_0}S_{\theta_0} - I_{xz}T_{\phi_0}S_{\phi_0}C_{\theta_0}\right)}{V_0}$$

$$[\boldsymbol{A}]_{pv} = \begin{bmatrix} C_{\theta_0} & S_{\phi_0}S_{\theta_0} & C_{\phi_0}S_{\theta_0} \\ 0 & C_{\phi_0} & -S_{\phi_0} \\ -S_{\theta_0} & S_{\phi_0}C_{\theta_0} & C_{\phi_0}C_{\theta_0} \end{bmatrix}$$

$$[\boldsymbol{A}]_{pe} = \begin{bmatrix} 0 & -V_0S_{\theta_0} & 0 \\ 0 & 0 & V_0C_{\theta_0} \\ 0 & -V_0C_{\theta_0} & 0 \end{bmatrix}$$

$$[\boldsymbol{A}]_{e\omega} = \begin{bmatrix} 1 & S_{\phi_0}T_{\theta_0} & C_{\phi_0}T_{\theta_0} \\ 0 & C_{\phi_0} & -S_{\phi_0} \\ 0 & \frac{S_{\phi_0}}{C_{\theta_0}} & \frac{C_{\phi_0}}{C_{\theta_0}} \end{bmatrix}$$

$$[\boldsymbol{A}]_{ee} = \begin{bmatrix} 0 & \frac{gT_{\phi_0}}{V_0C_{\theta_0}} & 0 \\ -\frac{gT_{\phi_0}C_{\theta_0}}{V_0} & 0 & 0 \\ 0 & \frac{gT_{\phi_0}T_{\theta_0}}{V_0} & 0 \end{bmatrix}$$

$$[\boldsymbol{C}]_f = \begin{bmatrix} 0 & X_{,\delta_e} & 0 \\ Y_{,\delta_a} & 0 & Y_{,\delta_r} \\ 0 & Z_{,\delta_e} & 0 \end{bmatrix}, \qquad [\boldsymbol{C}]_m = \begin{bmatrix} \ell_{,\delta_a} & 0 & \ell_{,\delta_r} \\ 0 & m_{,\delta_e} & 0 \\ n_{,\delta_a} & 0 & n_{,\delta_r} \end{bmatrix}$$

$$[\boldsymbol{i}] = \begin{bmatrix} 1 & 0 & 0 \\ 0 & 1 & 0 \\ 0 & 0 & 1 \end{bmatrix}, \qquad [\boldsymbol{n}] = \begin{bmatrix} 0 & 0 & 0 \\ 0 & 0 & 0 \\ 0 & 0 & 0 \end{bmatrix}$$

The system of linear equations that is presented in Eq. (18) can be used to study both turning and steady climbing flight along a linear flight path. With the equilibrium bank angle ϕ_0 set to zero, Eq. (18) provides the linearized equations of motion for linear climbing flight, including inertial, gyroscopic, and aerodynamic coupling. Steady level flight corresponds to the special case where both ϕ_0 and θ_0 are zero.

As can be seen from the formulation presented here, a wide range of longitudinal–lateral coupling is introduced by simple turning flight. Gyroscopic coupling enters the linearized equations of motion only through its effect on $[\boldsymbol{A}]_{m\omega}$ and, with no bank angle, inertial asymmetry produces coupling only through the moment of inertia tensor $[\boldsymbol{I}]$. Aerodynamic asymmetry typically produces significant coupling only through the stability tensor $[\boldsymbol{A}]_{mv}$. A nonzero bank angle, on the other hand, has broader effects on the linearized equations of motion. Turning flight introduces coupling in the translational velocity components as a result of the Coriolis forces seen in $[\boldsymbol{A}]_{fv}$. Additional translational coupling is introduced through the weight tensor $[\boldsymbol{A}]_w$, when the bank angle is nonzero. Turning also produces considerable rotational coupling as a result of the gyroscopic effects seen in $[\boldsymbol{A}]_{m\omega}$. Finally, turning produces coupling in the position and orientation equations through $[\boldsymbol{A}]_{pv}$, $[\boldsymbol{A}]_{e\omega}$, and $[\boldsymbol{A}]_{ee}$.

$$
\begin{bmatrix}
1-B_{x,\mu'} & 0 & -B_{x,\alpha'} & 0 & 0 & 0 & 0 & 0 & 0 & 0 & 0 & 0\\
0 & 1 & 0 & 0 & 0 & 0 & 0 & 0 & 0 & 0 & 0 & 0\\
-B_{z,\mu'} & 0 & 1-B_{z,\alpha'} & 0 & 0 & 0 & 0 & 0 & 0 & 0 & 0 & 0\\
0 & 0 & 0 & 1 & -\iota_{xy} & -\iota_{xz} & 0 & 0 & 0 & 0 & 0 & 0\\
-B_{m,\mu'} & 0 & -B_{m,\alpha'} & -\iota_{yx} & 1 & -\iota_{yz} & 0 & 0 & 0 & 0 & 0 & 0\\
0 & 0 & 0 & -\iota_{zx} & -\iota_{zy} & 1 & 0 & 0 & 0 & 0 & 0 & 0\\
0 & 0 & 0 & 0 & 0 & 0 & 1 & 0 & 0 & 0 & 0 & 0\\
0 & 0 & 0 & 0 & 0 & 0 & 0 & 1 & 0 & 0 & 0 & 0\\
0 & 0 & 0 & 0 & 0 & 0 & 0 & 0 & 1 & 0 & 0 & 0\\
0 & 0 & 0 & 0 & 0 & 0 & 0 & 0 & 0 & 1 & 0 & 0\\
0 & 0 & 0 & 0 & 0 & 0 & 0 & 0 & 0 & 0 & 1 & 0\\
0 & 0 & 0 & 0 & 0 & 0 & 0 & 0 & 0 & 0 & 0 & 1
\end{bmatrix}
\begin{Bmatrix}
\Delta\mu'\\ \Delta\beta'\\ \Delta\alpha'\\ \Delta\check{p}'\\ \Delta\check{q}'\\ \Delta\check{r}'\\ \Delta\varsigma_x'\\ \Delta\varsigma_y'\\ \Delta\varsigma_z'\\ \Delta\phi'\\ \Delta\theta'\\ \Delta\psi'
\end{Bmatrix}
=
\begin{bmatrix}
0 & D_{x,\delta_e} & 0\\
D_{y,\delta_a} & 0 & D_{y,\delta_r}\\
0 & D_{z,\delta_e} & 0\\
D_{\ell,\delta_a} & 0 & D_{\ell,\delta_r}\\
0 & D_{m,\delta_e} & 0\\
D_{n,\delta_a} & 0 & D_{n,\delta_r}\\
0 & 0 & 0\\
0 & 0 & 0\\
0 & 0 & 0\\
0 & 0 & 0\\
0 & 0 & 0\\
0 & 0 & 0
\end{bmatrix}
\begin{Bmatrix}
\Delta\delta_a\\ \Delta\delta_e\\ \Delta\delta_r
\end{Bmatrix}
$$

$$
+
\begin{bmatrix}
A_{x,\mu} & A_g S_{\phi_0} C_{\theta_0} & A_{x,\alpha} - A_g T_{\phi_0} S_{\phi_0} C_{\theta_0} & 0 & A_{x,\check{q}} & 0 & 0\,0\,0 & 0 & -A_g C_{\theta_0} & 0\\
-A_g S_{\phi_0} C_{\theta_0} & A_{y,\beta} & -A_g T_{\phi_0} S_{\theta_0} & A_{y,\check{p}} & 0 & A_{y,\check{r}} - 1 & 0\,0\,0 & A_g C_{\phi_0} C_{\theta_0} & -A_g S_{\phi_0} S_{\theta_0} & 0\\
A_{z,\mu} + A_g T_{\phi_0} S_{\phi_0} C_{\theta_0} & A_g T_{\phi_0} S_{\theta_0} & A_{z,\alpha} & 0 & A_{z,\check{q}} + 1 & 0 & 0\,0\,0 & -A_g S_{\phi_0} C_{\theta_0} & -A_g C_{\phi_0} S_{\theta_0} & 0\\
0 & A_{\ell,\beta} & A_{\ell,\alpha} & A_{\ell,\check{p}} + \eta_{xx} & -\eta_{xy} & A_{\ell,\check{r}} + \eta_{xz} & 0\,0\,0 & 0 & 0 & 0\\
A_{m,\mu} & A_{m,\beta} & A_{m,\alpha} & \eta_{yx} & A_{m,\check{q}} + \eta_{yy} & -\eta_{yz} & 0\,0\,0 & 0 & 0 & 0\\
0 & A_{n,\beta} & A_{n,\alpha} & A_{n,\check{p}} - \eta_{zx} & \eta_{zy} & A_{n,\check{r}} + \eta_{zz} & 0\,0\,0 & 0 & 0 & 0\\
C_{\theta_0} & S_{\phi_0} S_{\theta_0} & C_{\phi_0} S_{\theta_0} & 0 & 0 & 0 & 0\,0\,0 & 0 & -S_{\theta_0} & 0\\
0 & C_{\phi_0} & -S_{\phi_0} & 0 & 0 & 0 & 0\,0\,0 & 0 & 0 & C_{\theta_0}\\
-S_{\theta_0} & S_{\phi_0} C_{\theta_0} & C_{\phi_0} C_{\theta_0} & 0 & 0 & 0 & 0\,0\,0 & 0 & -C_{\theta_0} & 0\\
0 & 0 & 0 & 1 & S_{\phi_0} T_{\theta_0} & C_{\phi_0} T_{\theta_0} & 0\,0\,0 & 0 & A_g T_{\phi_0}/C_{\theta_0} & 0\\
0 & 0 & 0 & 0 & C_{\phi_0} & -S_{\phi_0} & 0\,0\,0 & -A_g T_{\phi_0} C_{\theta_0} & 0 & 0\\
0 & 0 & 0 & 0 & S_{\phi_0}/C_{\theta_0} & C_{\phi_0}/C_{\theta_0} & 0\,0\,0 & 0 & A_g T_{\phi_0} T_{\theta_0} & 0
\end{bmatrix}
\begin{Bmatrix}
\Delta\mu\\ \Delta\beta\\ \Delta\alpha\\ \Delta\check{p}\\ \Delta\check{q}\\ \Delta\check{r}\\ \Delta\varsigma_x\\ \Delta\varsigma_y\\ \Delta\varsigma_z\\ \Delta\phi\\ \Delta\theta\\ \Delta\psi
\end{Bmatrix}
\tag{24}
$$

Aerodynamic derivatives are usually specified in terms of dimensionless aerodynamic coefficients, and the linearized equations of motion are commonly solved in nondimensional form. By standard convention, the characteristic length used to nondimensionalize the longitudinal variables has been one-half the mean chord length. For the lateral variables, on the other hand, the wing semispan has traditionally been used as the characteristic length. When the longitudinal and lateral equations are uncoupled and solved separately, this duality presents no problem. However, in the coupled formulation presented here, longitudinal and lateral variables appear in the same equation, and it is quite inconvenient to use two different characteristic lengths. To nondimensionalize Eq. (18), it is convenient to select a single reference length for all longitudinal and lateral variables. With the equilibrium airspeed retained as the reference velocity, the usual nondimensional velocity disturbances remain,

$$\Delta\mu \equiv \Delta u/V_0, \qquad \Delta\beta \equiv \Delta v/V_0, \qquad \Delta\alpha \equiv \Delta w/V_0 \tag{19}$$

With the congruous reference length denoted as l_{ref}, the dimensionless angular rate disturbances are

$$\Delta\alpha' \equiv \Delta\dot{\alpha} l_{\text{ref}}/V_0, \qquad \Delta\check{p} \equiv \Delta p l_{\text{ref}}/V_0$$
$$\Delta\check{q} \equiv \Delta q l_{\text{ref}}/V_0, \qquad \Delta\check{r} \equiv \Delta r l_{\text{ref}}/V_0 \tag{20}$$

Similarly, the disturbances in aircraft position are nondimensionalized as

$$\Delta\varsigma_x \equiv \Delta x_c/l_{\text{ref}}, \qquad \Delta\varsigma_y \equiv \Delta y_c/l_{\text{ref}}, \qquad \Delta\varsigma_z \equiv \Delta z_c/l_{\text{ref}} \tag{21}$$

For dimensionless time we define

$$\tau \equiv V_0 t/l_{\text{ref}} \tag{22}$$

and

$$f' \equiv \frac{\partial f}{\partial \tau} = \frac{l_{\text{ref}}}{V_0}\frac{\partial f}{\partial t} \equiv \frac{l_{\text{ref}}}{V_0}\dot{f} \tag{23}$$

With these definitions, the nondimensional linearized equations of motion are

where

$$\iota_{xy} \equiv \frac{I_{xy}}{I_{xx}}, \qquad \iota_{xz} \equiv \frac{I_{xz}}{I_{xx}}, \qquad \iota_{yx} \equiv \frac{I_{xy}}{I_{yy}}, \qquad \iota_{yz} \equiv \frac{I_{yz}}{I_{yy}}$$

$$\iota_{zx} \equiv \frac{I_{xz}}{I_{zz}}, \qquad \iota_{zy} \equiv \frac{I_{yz}}{I_{zz}}, \qquad B_{x,\mu'} \equiv \frac{\rho S_w \bar{c}_w}{4W/g} C_{X,\hat{\mu}}$$

$$B_{z,\mu'} \equiv \frac{\rho S_w \bar{c}_w}{4W/g} C_{Z,\hat{\mu}}, \qquad B_{m,\mu'} \equiv \frac{\rho S_w \bar{c}_w^2 l_{\text{ref}}}{4I_{yy}} C_{m,\hat{\mu}}$$

$$B_{x,\alpha'} \equiv \frac{\rho S_w \bar{c}_w}{4W/g} C_{X,\hat{\alpha}}, \qquad B_{z,\alpha'} \equiv \frac{\rho S_w \bar{c}_w}{4W/g} C_{Z,\hat{\alpha}}$$

$$B_{m,\alpha'} \equiv \frac{\rho S_w \bar{c}_w^2 l_{\text{ref}}}{4I_{yy}} C_{m,\hat{\alpha}}, \qquad A_g \equiv \frac{g l_{\text{ref}}}{V_0^2}$$

$$\eta_{xx} \equiv A_g \frac{I_{xz} T_{\phi_0} S_{\phi_0} C_{\theta_0} - I_{xy} S_{\phi_0} C_{\theta_0}}{I_{xx}}$$

$$\eta_{xy} \equiv \frac{h_z l_{\text{ref}}}{I_{xx} V_0} + A_g \frac{(I_{zz} - I_{yy}) S_{\phi_0} C_{\theta_0} - 2 I_{yz} T_{\phi_0} S_{\phi_0} C_{\theta_0} + I_{xz} T_{\phi_0} S_{\theta_0}}{I_{xx}}$$

$$\eta_{xz} \equiv \frac{h_y l_{\text{ref}}}{I_{xx} V_0} + A_g \frac{(I_{yy} - I_{zz}) T_{\phi_0} S_{\phi_0} C_{\theta_0} - 2 I_{yz} S_{\phi_0} C_{\theta_0} + I_{xy} T_{\phi_0} S_{\theta_0}}{I_{xx}}$$

$$\eta_{yx} \equiv \frac{h_z l_{\text{ref}}}{I_{yy} V_0} + A_g \frac{(I_{zz} - I_{xx}) S_{\phi_0} C_{\theta_0} + 2 I_{xz} T_{\phi_0} S_{\theta_0} - I_{yz} T_{\phi_0} S_{\phi_0} C_{\theta_0}}{I_{yy}}$$

$$\eta_{yy} \equiv A_g \frac{I_{xy} S_{\phi_0} C_{\theta_0} + I_{yz} T_{\phi_0} S_{\theta_0}}{I_{yy}}$$

$$\eta_{yz} \equiv \frac{h_x l_{\text{ref}}}{I_{yy} V_0} + A_g \frac{(I_{zz} - I_{xx}) T_{\phi_0} S_{\theta_0} - 2 I_{xz} S_{\phi_0} C_{\theta_0} - I_{xy} T_{\phi_0} S_{\phi_0} C_{\theta_0}}{I_{yy}}$$

$$\eta_{zx} \equiv \frac{h_y l_{\text{ref}}}{I_{zz} V_0} + A_g \frac{(I_{yy} - I_{xx}) T_{\phi_0} S_{\phi_0} C_{\theta_0} + 2 I_{xy} T_{\phi_0} S_{\theta_0} - I_{yz} S_{\phi_0} C_{\theta_0}}{I_{zz}}$$

$$\eta_{zy} \equiv \frac{h_x l_{\text{ref}}}{I_{zz} V_0} + A_g \frac{(I_{yy} - I_{xx}) T_{\phi_0} S_{\theta_0} - 2 I_{xy} T_{\phi_0} S_{\phi_0} C_{\theta_0} - I_{xz} S_{\phi_0} C_{\theta_0}}{I_{zz}}$$

$$\eta_{zz} \equiv A_g \frac{-I_{yz} T_{\phi_0} S_{\theta_0} - I_{xz} T_{\phi_0} S_{\phi_0} C_{\theta_0}}{I_{zz}}$$

$$A_{x,\mu} \equiv \frac{\rho S_w l_{\text{ref}}}{2W/g} \left(2C_X + C_{X,\mu}\right), \qquad A_{z,\mu} \equiv \frac{\rho S_w l_{\text{ref}}}{2W/g} \left(2C_Z + C_{Z,\mu}\right)$$

$$A_{m,\mu} \equiv \frac{\rho S_w \bar{c}_w l_{\text{ref}}^2}{2I_{yy}} \left(2C_m + C_{m,\mu}\right), \qquad A_{x,\alpha} \equiv \frac{\rho S_w l_{\text{ref}}}{2W/g} C_{X,\alpha}$$

$$A_{z,\alpha} \equiv \frac{\rho S_w l_{\text{ref}}}{2W/g} C_{Z,\alpha}, \qquad A_{m,\alpha} \equiv \frac{\rho S_w \bar{c}_w l_{\text{ref}}^2}{2I_{yy}} C_{m,\alpha}$$

$$A_{y,\beta} \equiv \frac{\rho S_w l_{\text{ref}}}{2W/g} C_{Y,\beta}, \qquad A_{\ell,\beta} \equiv \frac{\rho S_w b_w l_{\text{ref}}^2}{2I_{xx}} C_{\ell,\beta}$$

$$A_{n,\beta} \equiv \frac{\rho S_w b_w l_{\text{ref}}^2}{2I_{zz}} C_{n,\beta}, \qquad A_{\ell,\alpha} \equiv \frac{\rho S_w b_w l_{\text{ref}}^2}{2I_{xx}} C_{\ell,\alpha}$$

$$A_{m,\beta} \equiv \frac{\rho S_w \bar{c}_w l_{\text{ref}}^2}{2I_{yy}} C_{m,\beta}, \qquad A_{n,\alpha} \equiv \frac{\rho S_w b_w l_{\text{ref}}^2}{2I_{zz}} C_{n,\alpha}$$

$$A_{y,\check{p}} \equiv \frac{\rho S_w b_w}{4W/g} C_{Y,\check{p}}, \qquad A_{\ell,\check{p}} \equiv \frac{\rho S_w b_w^2 l_{\text{ref}}}{4I_{xx}} C_{\ell,\check{p}}$$

$$A_{n,\check{p}} \equiv \frac{\rho S_w b_w^2 l_{\text{ref}}}{4I_{zz}} C_{n,\check{p}}, \qquad A_{x,\check{q}} \equiv \frac{\rho S_w \bar{c}_w}{4W/g} C_{X,\check{q}}$$

$$A_{z,\check{q}} \equiv \frac{\rho S_w \bar{c}_w}{4W/g} C_{Z,\check{q}}, \qquad A_{m,\check{q}} \equiv \frac{\rho S_w \bar{c}_w^2 l_{\text{ref}}}{4I_{yy}} C_{m,\check{q}}$$

$$A_{y,\check{r}} \equiv \frac{\rho S_w b_w}{4W/g} C_{Y,\check{r}}, \qquad A_{\ell,\check{r}} \equiv \frac{\rho S_w b_w^2 l_{\text{ref}}}{4I_{xx}} C_{\ell,\check{r}}$$

$$A_{n,\check{r}} \equiv \frac{\rho S_w b_w^2 l_{\text{ref}}}{4I_{zz}} C_{n,\check{r}}, \qquad D_{y,\delta_a} \equiv \frac{\rho S_w l_{\text{ref}}}{2W/g} C_{Y,\delta_a}$$

$$D_{\ell,\delta_a} \equiv \frac{\rho S_w b_w l_{\text{ref}}^2}{2I_{xx}} C_{\ell,\delta_a}, \qquad D_{n,\delta_a} \equiv \frac{\rho S_w b_w l_{\text{ref}}^2}{2I_{zz}} C_{n,\delta_a}$$

$$D_{x,\delta_e} \equiv \frac{\rho S_w l_{\text{ref}}}{2W/g} C_{X,\delta_e}, \qquad D_{z,\delta_e} \equiv \frac{\rho S_w l_{\text{ref}}}{2W/g} C_{Z,\delta_e}$$

$$D_{m,\delta_e} \equiv \frac{\rho S_w \bar{c}_w l_{\text{ref}}^2}{2I_{yy}} C_{m,\delta_e}, \qquad D_{y,\delta_r} \equiv \frac{\rho S_w l_{\text{ref}}}{2W/g} C_{Y,\delta_r}$$

$$D_{\ell,\delta_r} \equiv \frac{\rho S_w b_w l_{\text{ref}}^2}{2I_{xx}} C_{\ell,\delta_r}, \qquad D_{n,\delta_r} \equiv \frac{\rho S_w b_w l_{\text{ref}}^2}{2I_{zz}} C_{n,\delta_r}$$

Here $\hat{\mu}$ and $\hat{\alpha}$ are used to signify the traditional nondimensional accelerations.

Even for the special case of linear flight with no coupling, Eq. (24) can be efficiently used to obtain the eigenvalues and eigenvectors for both longitudinal and lateral motion. When the bank angle and all coupling terms are zero, results obtained from Eq. (24) are identical to those obtained from the traditional uncoupled formulation. The only advantage to be gained from using the uncoupled formulation in place of Eq. (24) is computational efficiency. Two 6×6 eigenproblems can be numerically solved slightly faster than one 12×12 eigenproblem. However, with the computational hardware and software available today, when solving something as simple as a 12×12 eigenproblem, it typically takes longer to display the results than it does to perform the numerical computations. Thus, with problems of this level of complexity, computation time is no longer an issue. With current computational tools, the advantages of being able to account for inertial, gyroscopic, and aerodynamic coupling, as well as turning flight, far outweigh any computational advantage of using the uncoupled equations for longitudinal and lateral motion. Therefore, when developing computer code for today's hardware, Eq. (24) provides significant advantage over the traditional uncoupled formulation.

Aerodynamic coupling between the longitudinal and lateral modes is embodied in the linearized formulation through the inclusion of additional aerodynamic derivatives, which are not included in the traditional formulation. In the present formulation three additional aerodynamic derivatives have been included: the change in rolling moment coefficient with angle of attack, $C_{\ell,\alpha}$; the change in yawing moment coefficient with angle of attack, $C_{n,\alpha}$; and the change in pitching moment coefficient with sideslip angle, $C_{m,\beta}$. These three derivatives were included in the present formulation because they are the coupling derivatives that most commonly become significant when an airplane is flown in an asymmetric configuration. This type of aerodynamic coupling is produced by a rotating propeller and can also occur whenever an aircraft is flown with an asymmetric distribution of external stores attached to the wings. This does not imply that the other longitudinal–lateral coupling derivatives are always insignificant. Additional aerodynamic coupling derivatives can easily be added to the formulation presented here. For example, the term to account for the change in pitching moment with rolling rate could be added to the fourth column of the fifth row in the stiffness matrix on the right-hand side of Eq. (24). Similarly, a change in the aerodynamic yawing moment with forward airspeed could easily be added to the first column of the sixth row and so on. Once the first coupling term is included, adding others does not significantly increase the complexity.

Using the nondimensional linearized formulation that was presented here requires the specification of a single congruous reference length for both the longitudinal and lateral variables. The choice of this reference length is quite arbitrary. The choice has no effect on the predicted dynamics, if the reference length is used consistently. A reasonable choice might be the square root of the wing planform area.

Example Results

Perhaps the most common cause of aerodynamic coupling between the longitudinal and lateral modes is simply a rotating propeller. No propeller-driven aircraft can be truly symmetric, unless it has an even number of counter-rotating propellers symmetrically distributed in the spanwise direction. An aircraft with a single rotating propeller will always display some degree of aerodynamic coupling between the longitudinal and lateral modes. This is partially due to the fact that a rotating propeller produces a yawing moment that is proportional to the propeller angle of attack. In addition, a single rotating propeller will always produce some gyroscopic coupling. For conventional propeller-driven airplanes with low power-to-weight ratio, these effects are not too significant. However, a single-engine propeller-driven airplane with very high power-to-weight ratio can exhibit longitudinal–lateral coupling that substantially alters the dynamics of the aircraft. One example of such an airplane is the British Spitfire Mark XVIII, shown in Fig. 2. To

Table 1 Comparison between the level-flight eigenvalues, with and without coupling introduced by the rotating propulsion system

	Without coupling		With coupling	
Mode	Period, s	Damping rate, s^{-1}	Period, s	Damping rate, s^{-1}
Phugoid	66.7	0.0133	71.0	0.0132
Short period	1.67	2.84	1.42	1.81
Dutch roll	1.55	0.571	1.72	1.59
Roll	∞	51.3	∞	51.3
Spiral	∞	−0.0030	∞	−0.0031

Fig. 2 British Spitfire Mark XVIII used for the example computations (photograph by Barry Santana).

demonstrate how longitudinal–lateral coupling can affect aircraft dynamics, results of some example computations for this aircraft will be presented.

For the computational results presented here, the aerodynamic derivatives for the Spitfire were predicted analytically from known dimensions, weights, and power. Although the derivatives so predicted are not expected to exactly match the aerodynamics of the actual aircraft, they are certainly reasonable and adequate for the demonstration purposes intended here. The Spitfire Mark XVIII shown in Fig. 2 is powered by a liquid-cooled, 12-cylinder, Rolls-Royce Griffon engine developing 2375 hp at 2750 rpm. The 132-in., five-blade, Rotol propeller is turned with 1.961–1 gear reduction. The airplane has a top speed in level flight of 450 mph and has a rate of climb at sea level of over 5000 ft/min. The mass moment of inertia for the crankshaft, hub, and propeller combined was estimated at approximately 86 slug · ft^2. For the following results, an airspeed of 300 mph at sea level was used, and the engine was assumed to be turning at 2600 rpm. From the propeller geometry and assumed operating conditions, a numerical procedure[10] based on Goldstein's vortex theory[11] was used to estimate the change in propeller yawing moment with angle of attack. From this result, the change in airplane yawing moment coefficient with angle of attack was estimated to be about $C_{n,\alpha} = +0.034$, and the change in pitching moment coefficient with sideslip angle was approximated at $C_{m,\beta} = +0.16$. (The Griffon engine has left-hand rotation.) With the exception of the rotating propeller and crankshaft, the airplane was assumed to be completely symmetric in the spanwise direction.

Table 1 shows a comparison between the rigid-body eigenvalues for the Spitfire as predicted from Eq. (24), both excluding and including the gyroscopic and aerodynamic coupling generated by the rotating propeller and crankshaft. The results presented in Table 1 are for level flight at sea level with an airspeed of 440 ft/s. Notice that longitudinal–lateral coupling has the greatest effect on the damping for the short-period and Dutch roll modes. The roll and spiral modes are almost totally unaffected by the coupling.

The effect of coupling on the short-period and Dutch roll modes is even more dramatically demonstrated by examining the eigenvectors. Table 2 shows the short-period and Dutch roll eigenvectors, as predicted from Eq. (24) with the gyroscopic and aerodynamic coupling terms set to zero. Here we see traditional results, where the short-period mode involves only longitudinal disturbances and Dutch roll involves only lateral disturbances. As expected from a traditional viewpoint, the short-period mode involves oscillations

Table 2 Short-period and Dutch roll level-flight eigenvectors, excluding coupling introduced by the rotating propulsion system

Eigenvector component	Short period		Dutch roll	
	Amplitude	Phase, deg	Amplitude	Phase, deg
$\Delta\mu$	0.0027	80.24	0.0000	0.00
$\Delta\beta$	0.0000	0.00	0.6967	−178.31
$\Delta\alpha$	0.3037	72.46	0.0000	0.00
$\Delta\check{p}$	0.0000	0.00	0.0042	100.66
$\Delta\check{q}$	0.0415	169.08	0.0000	0.00
$\Delta\check{r}$	0.0000	0.00	0.1016	97.89
$\Delta\varsigma_x$	0.0163	−46.62	0.0000	0.00
$\Delta\varsigma_y$	0.0000	0.00	0.1249	178.08
$\Delta\varsigma_z$	0.9188	0.00	0.0000	0.00
$\Delta\phi$	0.0000	0.00	0.0290	2.77
$\Delta\theta$	0.2482	42.23	0.0000	0.00
$\Delta\psi$	0.0000	0.00	0.6985	0.00

Table 3 Short-period and Dutch roll level-flight eigenvectors, including coupling introduced by the rotating propulsion system

Eigenvector component	Short period		Dutch roll	
	Amplitude	Phase, deg	Amplitude	Phase, deg
$\Delta\mu$	0.0031	68.88	0.0029	62.64
$\Delta\beta$	0.2675	78.84	0.2196	46.41
$\Delta\alpha$	0.2842	42.64	0.2122	45.58
$\Delta\check{p}$	0.0019	13.16	0.0013	−18.76
$\Delta\check{q}$	0.0459	125.13	0.0287	123.19
$\Delta\check{r}$	0.0455	9.93	0.0310	−21.40
$\Delta\varsigma_x$	0.0179	−43.20	0.0201	−50.76
$\Delta\varsigma_y$	0.0329	49.45	0.0390	11.67
$\Delta\varsigma_z$	0.8354	0.00	0.9023	0.00
$\Delta\phi$	0.0109	−98.91	0.0090	−132.16
$\Delta\theta$	0.2697	13.05	0.2024	9.79
$\Delta\psi$	0.2668	−102.14	0.2186	−134.80

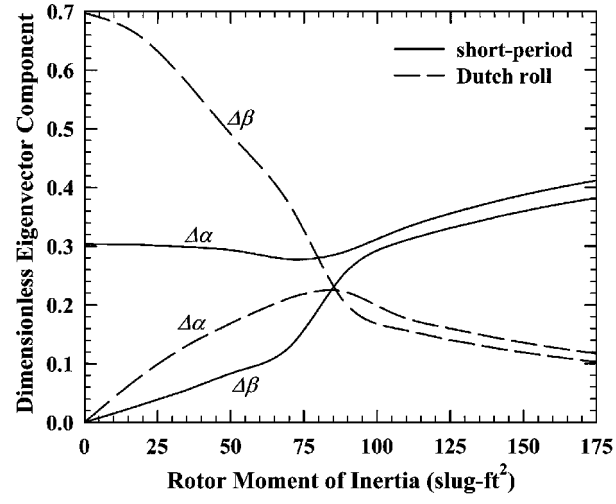

Fig. 3 Variation with gyroscopic coupling in the angle-of-attack and sideslip components for the short-period and Dutch roll eigenvectors, excluding the aerodynamic coupling terms.

in angle of attack but no oscillations in sideslip. Dutch roll, on the other hand, produces oscillations in sideslip with no oscillations in angle of attack. A substantially different result is seen in Table 3, which was predicted from Eq. (24), including the gyroscopic and aerodynamic coupling terms. Here we see that both modes exhibit oscillations in angle of attack and sideslip that are of almost equal magnitude. Neither of these two modes is readily identifiable as being either longitudinal or lateral. In fact, the authors were able to identify the short-period and Dutch roll modes in Table 3 only by incrementally varying the magnitude of the coupling terms and observing the transition between the results shown in Table 2 and those shown in Table 3.

To give the reader a better feel for how the eigenvectors change with increasing longitudinal–lateral coupling, Fig. 3 shows the

Table 4 Comparison between the eigenvalues for a 60-deg coordinated turn, with and without the coupling introduced by the rotating propulsion system

	Without coupling		With coupling	
Mode	Period, s	Damping rate, s^{-1}	Period, s	Damping rate, s^{-1}
Phugoid	38.5	0.0039	38.0	0.0032
Short period	1.67	2.84	1.42	1.82
Dutch roll	1.55	0.572	1.72	1.59
Roll	∞	51.3	∞	51.3
Spiral	∞	0.0211	∞	0.0230

angle-of-attack and sideslip components for both the short-period and Dutch roll eigenvectors. For the results shown in Fig. 2, the aerodynamic coupling terms were set to zero and the moment of inertia for the propeller and crankshaft was varied from zero to more than twice that estimated for the actual airplane. The rotational speed of the engine and all other parameters in Eq. (24) were held constant. When the rotor moment of inertia is set to zero, there is no gyroscopic coupling, and the Dutch roll and short-period modes take traditional form. In this case, shown on the far left-hand side of Fig. 3, the short-period mode includes no sideslip, and Dutch roll involves no changes in angle of attack. As the rotor moment of inertia and corresponding gyroscopic coupling are increased, the Dutch roll oscillations in angle of attack and the short-period oscillations in sideslip begin to increase. With a rotor moment of inertia in the range of that estimated for the actual airplane ($86\ \text{slug} \cdot \text{ft}^2$), the magnitude of the oscillation in angle of attack and sideslip are about the same for both the short-period and Dutch roll modes. For very high levels of gyroscopic coupling, as shown on the right-hand side of Fig. 3, the short-period oscillations in sideslip become significantly larger than those for Dutch roll, and the Dutch roll oscillations in angle of attack are somewhat greater than those in sideslip. With high levels of gyroscopic coupling, the characteristics of Dutch roll and the short-period mode seem to be dominated by gyroscopic effects.

Turning flight can also affect the classical modes of a conventional airplane, even when the other forms of longitudinal–lateral coupling are not significant. Table 4 shows a comparison between the rigid-body eigenvalues for the Spitfire Mark XVIII in turning flight, both excluding and including the gyroscopic and aerodynamic coupling generated by the rotating propeller and crankshaft. The results presented in Table 4 were predicted from Eq. (24) for a level coordinated turn at sea level, using an airspeed of 440 ft/s and a bank angle of 60 deg. Notice, by comparison of the results in Table 4 with those in Table 1, that turning flight has almost no effect on the short-period and Dutch roll modes. Within the three significant digits that are reported in Tables 4 and 1, Dutch roll and the short-period modes display only two minor differences between the 60-deg banked turn and level flight. These are in the short-period damping with coupling and in the Dutch roll damping without coupling. Clearly, these two small differences are not significant. On the other hand, the phugoid and spiral modes are seen to be substantially affected by the turn, even when the gyroscopic and aerodynamic coupling is ignored. As a result of the turn, the phugoid period was nearly cut in half, and the damping was reduced by more than a factor of three. For the spiral mode, the turn increased the damping rate by 800 %, changing the mode from slowly divergent to convergent.

Conclusions

From the results presented here, we see that turning flight and other forms of longitudinal–lateral coupling can have a significant effect on aircraft dynamics. When the longitudinal–lateral coupling terms in Eq. (24) are present but small, all of the traditional longitudinal and lateral modes are still observed in the solution to the associated eigenproblem. The net effect of a small amount of coupling is to produce modest changes in the frequencies and damping rates associated with the traditional modes, while introducing some lateral motion into the longitudinal modes and vice versa. This is the case that most accurately describes the majority of conventional airplanes with low power-to-weight ratio. At least a small amount of longitudinal–lateral coupling is usually present in any aircraft. If the coupling terms in Eq. (24) become large enough, the interactions between the longitudinal and lateral DOF can be sufficient to render the traditional longitudinal and lateral modes unrecognizable.

A single-engine propeller-driven airplane with very high power-to-weight ratio can exhibit significant longitudinal–lateral coupling. The British Spitfire Mark XVIII used for the example computations was chosen specifically because it displays such characteristics. Whereas the level-flight dynamics of most conventional airplanes with low power-to-weight ratio is not significantly affected by longitudinal–lateral coupling, there have been and will continue to be applications where this effect is substantial. Furthermore, the longitudinal–lateral coupling associated with turning flight can significantly alter the phugoid and spiral modes of any aircraft.

There is also a fairly new area within the field of flight mechanics where longitudinal–lateral coupling may become important. This is in the area of microflight. Recent developments in the field of nanotechnology have sparked interest in flight on a very small scale. As this new technology develops, we may find that the dynamic characteristics of some of these tiny aircraft are dominated by longitudinal–lateral coupling. Even if this does not prove to be the case, it should be investigated. Furthermore, because the linearized formulation presented here is not significantly more complex than the traditional linearized formulation, longitudinal–lateral coupling can be accounted for as easily as it can be ignored.

References

[1]Nelson, R. C., "Small-Disturbance Theory," *Flight Stability and Automatic Control*, 2nd ed., McGraw–Hill, New York, 1998, pp. 104–108.

[2]Pamadi, B. N., "Equations of Motion with Small Disturbances," *Performance, Stability, Dynamics, and Control of Airplanes*, AIAA, Reston, VA, 1998, pp. 372–375.

[3]Etkin, B., and Reid, L. D., "The Small-Disturbance Theory," *Dynamics of Flight: Stability and Control*, 3rd ed., Wiley, New York, 1996, pp. 107–114.

[4]McRuer, D. T., Ashkenas, I. L., and Graham, D., "Complete Linearized Equations of Motion," *Aircraft Dynamics and Automatic Control*, Princeton Univ. Press, Princeton, NJ, 1973, pp. 255–262.

[5]Etkin, B., "The Small-Disturbance Theory," *Dynamics of Atmospheric Flight*, Wiley, New York, 1973, pp. 154–165.

[6]Bryan, G. H., *Stability in Aviation*, MacMillan, London, 1911.

[7]Nelson, R. C., "Inertial Coupling," *Flight Stability and Automatic Control*, 2nd ed., McGraw–Hill, New York, 1998, pp. 205, 206.

[8]Etkin, B., and Reid, L. D., "Effect of Spinning Rotors on the Euler Equations," *Dynamics of Flight: Stability and Control*, 3rd ed., Wiley, New York, 1996, pp. 103–103.

[9]Phillips, W. F., Hailey, C. E., and Gebert, G. A., "A Review of Attitude Representations Used for Aircraft Kinematics," *Journal of Aircraft*, Vol. 38, No. 4, 2001, pp. 718–737.

[10]Phillips, W. F., and Anderson, E. A., "Predicting the Contribution of Running Propellers to Aircraft Stability Derivatives," AIAA Paper 2002-0390, 2002.

[11]Goldstein, S., "On the Vortex Theory of Screw Propellers," *Proceedings of the Royal Society*, Series A: Mathemetical and Physical Sciences, Vol. 123, 1929, pp. 440–465.